

Analysis and Study of the Impact of Upgrading the Treatment Head of Elekta Precise Linear Accelerator on the Beam Profile Parameters of 6 MV and 15 MV Photon Beams.

¹Abdurraouf M. Aghila, ¹Ali R. Khalf, ²Faraj A. Elmasrub

¹Physics Department, Faculty of Education-Tripoli, University of Tripoli, Tripoli, Libya.

²National Cancer Institute of Sabratha, Sabratha, Libya.

*Corresponding: ab.aghila@uot.edu.ly

دراسة وتحليل تأثير تطوير رأس جهاز المعجل الخطي Elekta Precise على معاملات المقطع الجانبي لحزم الفوتونات ذات الطاقة 6 MV و 15 MV.

Article history

Received: Nov 5, 2024

Accepted: Nov 27, 2024

الملخص:

يلعب العلاج الإشعاعي دورًا حاسمًا في علاج الأورام الخبيثة، حيث يعمل كطريقة علاج أساسية أو مساعدة لحوالي 50% من مرضى الأورام السرطانية. للحصول على نتائج مثالية، يجب أن لا تتجاوز جرعات الإشعاع الموصوفة والواصلة لحجم الهدف المخطط له $\pm 5\%$. تبحث هذه الدراسة في تأثير تطوير المعجل الخطي (Elekta Precise) بقسم العلاج الإشعاعي بمستشفى طرابلس الجامعي في طرابلس، ليبيا، من رأس إشعاع قياسي (SH) إلى رأس متعدد الشرائح (MLC) على خصائص حزم الفوتونات، وتحديدًا بارمترات المقاطع الجانبية للإشعاع لطاقات 6 MV و 15 MV. باستخدام نظام المسح الثلاثي الأبعاد PTW MP3-M، تشمل القياسات الإشعاعية تسطح حزمة الإشعاع والتناظر وشبه الظل قبل وبعد تطوير الجهاز لحقول علاجية وأعماق مختلفة. كشفت نتائج هذه الدراسة عن اختلاف كبير في بارمترات المقاطع الجانبية للإشعاع بعد تطوير جهاز المعجل حيث كانت الاختلافات النسبية في تسطح حزمة الإشعاع 66.30% لحزمة الفوتونات 6 MV و 24.64% لحزمة الفوتونات 15 MV. إضافة إلى ذلك، كان أعلى اختلاف نسبي مسجل في طول منطقة شبه الظل 31.76% لطاقة الفوتونات 6 MV و 17.65% لطاقة الفوتونات 15 MV. وبالتالي، فمن الضروري والموصى به بشدة إعادة إجراء قياسات بيانات بداية التشغيل للمقاطع الجانبية للإشعاع والتي يتم استخدامها في أنظمة تخطيط العلاج للتنبؤ بتوزيع الجرعة لدى المرضى.

الكلمات المفتاحية: المقاطع الجانبية للإشعاع، محدد متعدد الشرائح، محدد قياسي، التسطح، التماثل، شبه الظل، Elekta Precis Linac.

ABSTRACT:

Radiotherapy plays a crucial role in the management of malignant tumors, serving as an essential or adjunct treatment modality for approximately 50% of cancer patients. For optimal outcomes, the prescribed and delivered radiation doses to the planning target volume must align within $\pm 5\%$. This study investigates the impact of upgrading the Elekta Precise Linear Accelerator (LINAC) at the Radiotherapy Department of Tripoli University Hospital in Tripoli, Libya, from a standard radiation head (SH) to a multileaf collimator (MLC) head on photon beam characteristics, specifically the beam profile parameters for energies of 6 MV and 15 MV. Utilizing a PTW MP3-M 3D water scanning system, detailed dosimetric measurements—including beam flatness, symmetry, and penumbra—were conducted before and after the upgrade across various field sizes and depths. The results of this study reveal a significant difference in beam profile parameters post-upgrade. The relative differences in beam flatness were 66.30% for the 6 MV beam and 24.64% for the 15 MV beam. Additionally, the highest recorded relative difference in beam penumbra was 31.76% for the 6 MV beam energy and 17.65% for the 15 MV beam energy. Consequently, it is essential and strongly recommended that the collected beam profile data be recommissioned since it is provided to the treatment planning system used to predict dose distribution in cancer patients.

Keywords: Beam Profile, MLC, SH Collimator, Flatness, Symmetry, Penumbra, Elekta Precis Linac.

Introduction:

Currently, radiotherapy is one of the most commonly used oncological therapies in the treatment of malignant tumors. Furthermore, it is considered an essential or complementary part of treatment in approximately 50% of cancer patients [1,2,3]. For



radiotherapy to be effective and achieve a controlled cure rate without excessive healthy tissue complications, the prescribed and delivered dose to a planning target volume (PTV) must agree within $\pm 5\%$ [4, 5, 6]. The delivered radiation dose is influenced by several factors, some are related to tumor specifications, while others are associated with the radiation machine used. The Linear accelerator has been a vital tool in contemporary external beam radiation therapy since 1953 [7]. The design of Linear accelerators can vary between manufacturers in terms of the specific components used, the overall layout of the machine, and the control systems employed. Different manufacturers may prioritize different features or technologies in their designs, leading to variations in performance and capabilities [8, 9, 10].

The year 2013 witnessed an upgrade of the first linear accelerator (LINAC) machine installed in the Radiotherapy Department at Tripoli University Hospital (TUH) in Libya during the year 2004. The machine was an Elekta Precise LINAC with multiple photon and electron beam energies and a standard radiation head (SH) with asymmetric jaws. The upgrade involves replacing the SH with a multileaf collimator head (MLC) to define the radiation field geometry. The new head has two banks, each containing 40 leaves with a nominal width projection of 10 mm at the isocenter [11]. The design of the treatment head of a LINAC has a significant influence on the dose distribution. Since the radiation dose distribution is influenced by the characteristics of the radiation beam, such as the percentage depth dose and beam profile, variations in this quantity are expected due to the upgrade that the LINAC has undergone. According to Task Group 53 [12] of the American Association of Physicists in Medicine, the machine should be recommissioned after significant maintenance, adjustments, or other alterations to the beam modifications. Additionally, the results of Aghila et al [13]. in their study of the impact of upgrading the LINAC showed significant differences in percentage depth dose parameters. Therefore, this study aimed to examine and assess the impacts of upgrading the Elekta Precise LINAC on the beam profile parameters for photon beams of energies 6 MV and 15 MV. The investigation involved detailed measurements and analyses of the beam profiles before and after the upgrade. Various dosimetric parameters of the beam profile, such as beam flatness, symmetry, and penumbra, were evaluated to quantify the changes resulting from the enhancements.

Materials and Methods:

An Elekta Precise linear accelerator (Elekta Ltd., Crawley, UK) with two treatment modes, photon and electron beams, was employed for the measurements in this study. The photon mode energies were 4 MV, 6 MV, and 15 MV before the upgrade, and they were 6 MV, 10 MV, and 15 MV beam energies following the upgrade. However, the electron mode energies were 4 MeV, 6 MeV, 8 MeV, 10 MeV, 15 MeV, and 18 MeV before the upgrade, while after the upgrade, the energy of 12 MeV was added to the previous energies.

The beam profile measurements were obtained using a motorized PTW MP3-M 3D water scanning system (PTW, Freiburg, Germany), a water tank of inner size 59.6 cm × 59.4 cm × 50.25 cm, a TANDEM electrometer, a TBA control unit, and two 0.125 cm³ Semiflex ionization chambers for in-field and reference. MEPHISTO mc² navigation software (PTW, Freiburg) version 1.6 was used for data processing and analysis. The measurements of beam profile pre- and post-upgrade were conducted at a constant source-to-surface distance of 100 cm for various field sizes ranging from 3 × 3 cm² to 35 × 35 cm² at specific depths (depth of maximum dose cm (d_{max}), 5 cm, 10 cm, 20 cm, and 30 cm). The angles of the gantry and the collimator were at 0° during the measurements. The International Atomic Energy Agency (IAEA) Technical Report Series 277 and 398 dosimetry protocols [14, 15] were followed for the beam profile measurements.

Results and Discussion:

The beam profile, which is the absorbed dose distribution at a given depth in water phantom parallel to the water surface and perpendicular to the beam central axis [16, 17], is influenced by the primary of accelerated electron, thickness, and atomic number of target that the accelerated electrons collide with, and the flattening filter [18]. It should be noted that the data on radiation dose distribution along the central and off-axis, together with other parameter measurements, are essential for predicting the radiation dose within patients via the treatment planning systems [19]. For calculations of beam flatness, beam symmetry, and beam penumbra, the beam profiles were normalized to 100% at the central axis to their corresponding field sizes. The relative difference (RD) between the parameter values pre- and post-upgrade was calculated using the following formula:

$$RD = \frac{|V_1 - V_2|}{(V_1 + V_2)/2} \times 100$$

Where: V_1 the value pre-upgrade, V_2 the value post-upgrade.

Beam profile:

Beam profile measurements for selected field sizes ($5 \times 5 \text{ cm}^2$, $10 \times 10 \text{ cm}^2$, $20 \times 20 \text{ cm}^2$, and $30 \times 30 \text{ cm}^2$) of energies 6 MV and 15 MV are presented in Figures 1 and 2, respectively. The profiles were measured at depths of depth of dose maximum d_{max} cm, 5 cm, 10 cm, 20 cm, and 30 cm.

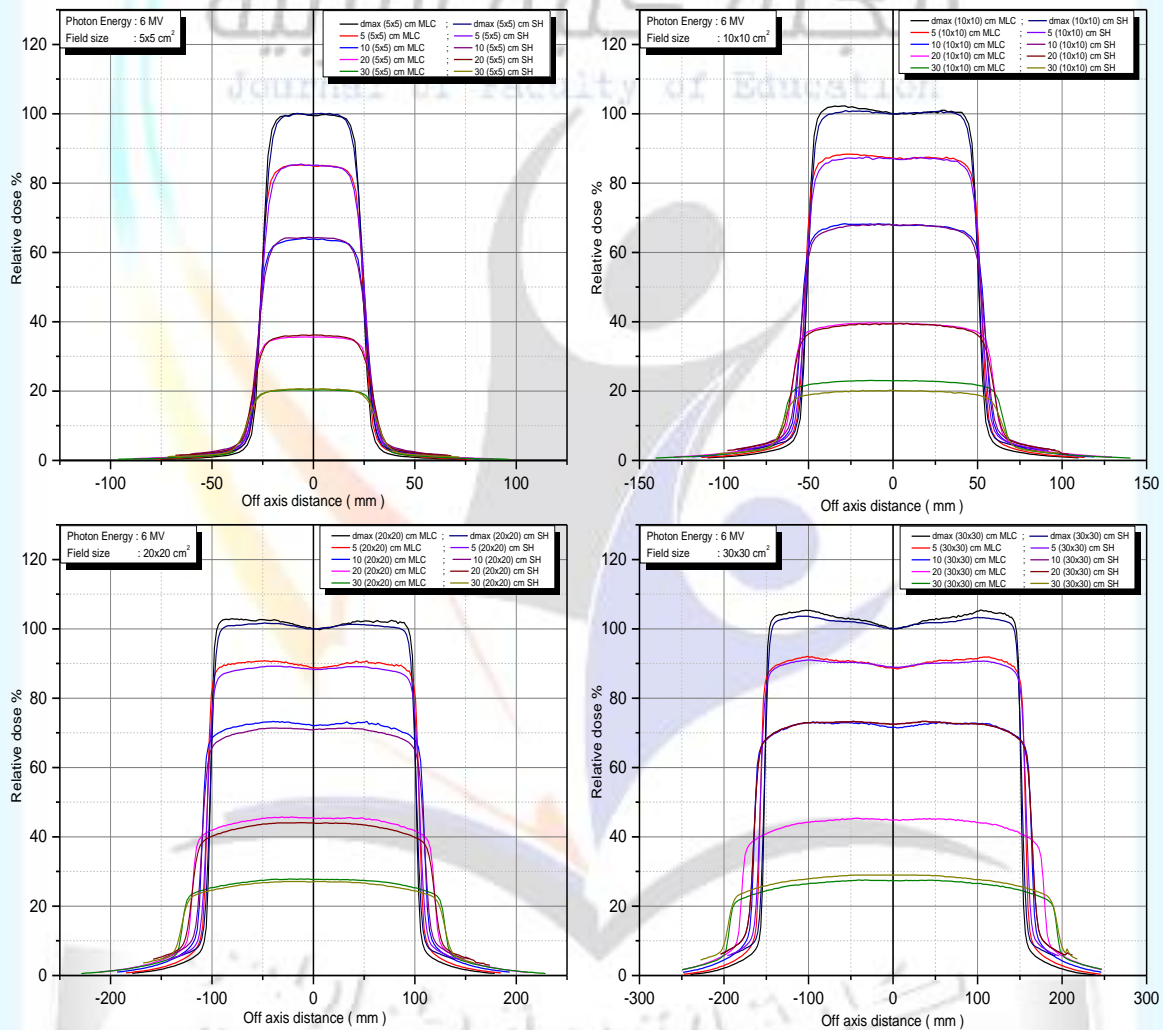


Figure 1: Beam profiles of size $5 \times 5 \text{ cm}^2$, $10 \times 10 \text{ cm}^2$, $20 \times 20 \text{ cm}^2$ and $30 \times 30 \text{ cm}^2$ for photon energy of 6 MV.

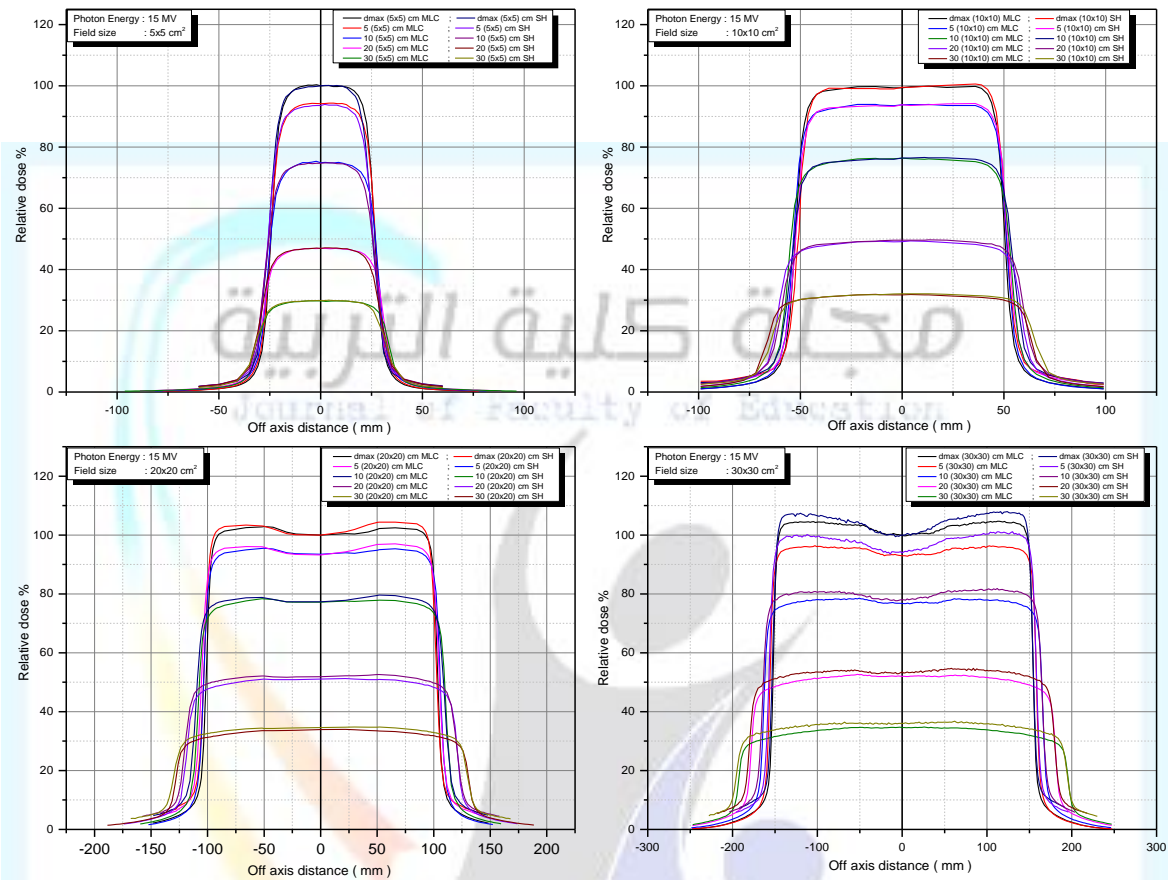


Figure 2: Beam profiles of size $5 \times 5 \text{ cm}^2$, $10 \times 10 \text{ cm}^2$, $20 \times 20 \text{ cm}^2$ and $30 \times 30 \text{ cm}^2$ for photon energy of 15 MV.

Figures 1 and 2 illustrate a well-distribution of radiation dose on both sides of the central axis. The radiation dose is uniformly distributed and then decreases towards the edges to form a penumbra region.

Measured field size:

Figures 3 and 4 illustrate a detailed analysis of the percentage difference in field sizes for 6 MV and 15 MV photon beams, respectively, following an upgrade in collimation technology. Figure 3 shows that the 6 MV photon beam has minimal variations, with differences ranging from 0.1% to 1.77% across different field sizes. On the other hand, Figure 4 indicates larger differences for the 15 MV beam, ranging from 2.1% to 3.3%, highlighting that collimation system effects are more significant at higher energy levels.

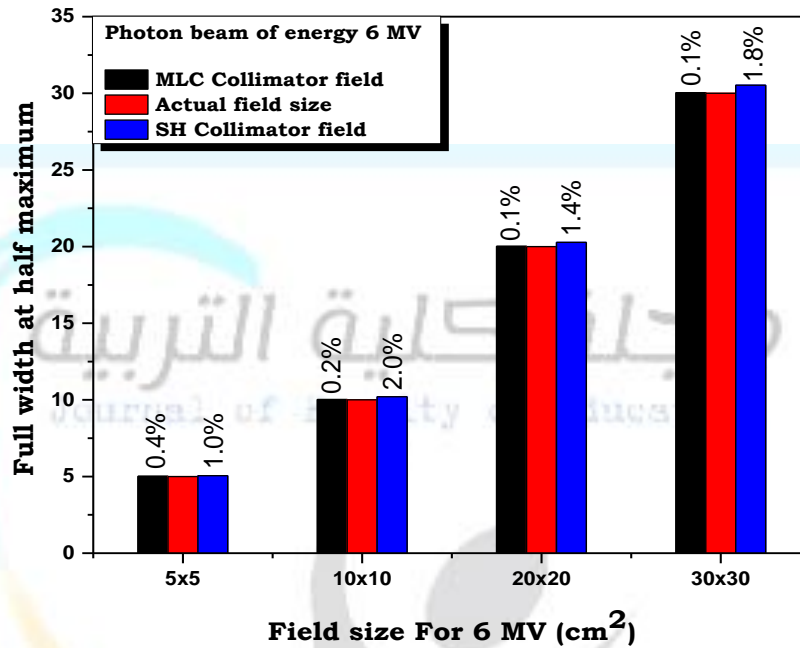


Figure 3: Nominal field size vs measured FWHM for photon energy of 6 MV.

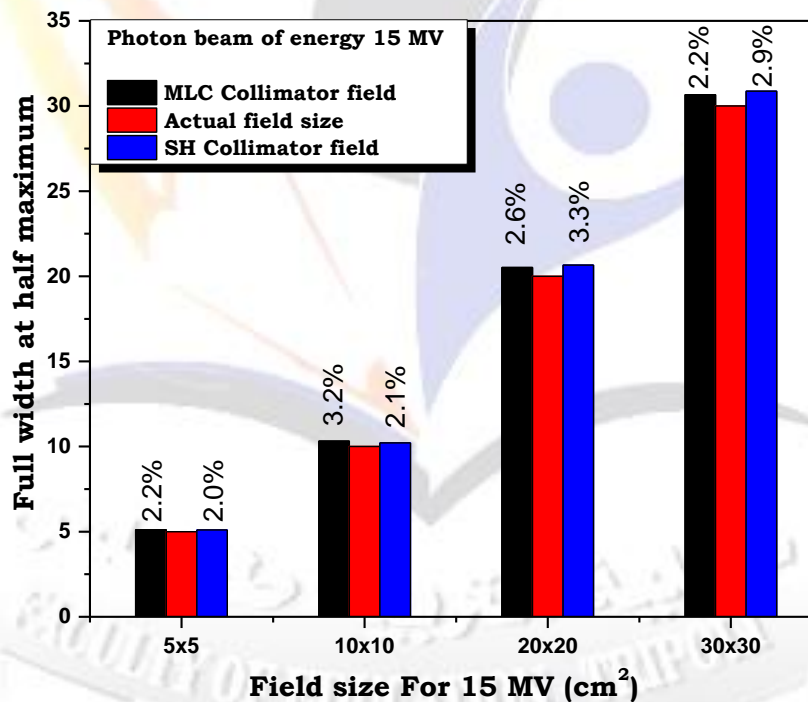


Figure 4: Nominal field size vs measured FWHM for photon energy of 15 MV.

Beam flatness:

The results of beam flatness values of 6 MV and 15 MV photon beam energies measured at various depths (d_{max} cm, 5 cm, 10 cm, 20 cm, and 30 cm) and field sizes (5x5

cm², 10×10 cm², 20×20 cm², and 30×30 cm²), for both the SH and the ML Collimators, are presented in Tables 1 and 2, respectively. Table 3 shows the Relative difference (RD) in beam flatness values between the SH and ML collimators across two distinct photon beam energies: 6 MV and 15 MV.

Table 1: represent the beam flatness values of 6 MV beam energy at various depths and field sizes for both the SH and ML collimator.

Field size	Collimator type	Depth (cm)				
		d _{max}	5	10	20	30
5x5 cm ²	ML Collimator	2.42	3.2	3.56	3.68	3.83
	SH Collimator	4.82	5.31	5.73	5.92	6.16
10x10 cm ²	ML Collimator	0.77	1.39	1.97	2.87	3.5
	SH Collimator	1.11	1.81	2.52	3.63	4.12
20x20 cm ²	ML Collimator	1.56	1.83	1.93	3.89	5.28
	SH Collimator	1.07	1.28	2.23	4.36	5.82
30x30 cm ²	ML Collimator	1.31	1.57	1.95	4.31	6.45
	SH Collimator	1.00	1.23	1.82	4.51	6.73

Table 2: represent the beam flatness values of 15 MV beam energy at various depths and field sizes for both the SH and ML collimator.

Field size	Collimator type	Depth (cm)				
		d _{max}	5	10	20	30
5x5 cm ²	ML Collimator	4.84	5.44	5.58	5.02	5.29
	SH Collimator	6.20	6.25	6.43	6.52	6.61
10x10 cm ²	ML Collimator	1.04	1.59	2.28	2.98	3.41
	SH Collimator	1.30	1.7	2.3	3	3.4
20x20 cm ²	ML Collimator	1.24	1.57	1.72	2.39	3.15
	SH Collimator	2.14	2.41	2.38	2.73	3.72
30x30 cm ²	ML Collimator	1.49	1.89	2.26	3.27	5.13
	SH Collimator	3.85	3.95	4.41	4.49	5.47

Table 3: represent the relative difference in beam flatness values between the Jaw collimator and Multileaf collimators for 6 MV and 15 MV photon beam energies.

Beam energy	Field size (cm ²)	Depth (cm)				
		d _{max}	5	10	20	30
6 MV	5x5	66.3%	49.59%	46.72%	46.67%	46.65%
	10x10	36.17%	26.25%	24.5%	23.38%	16.27%
	20x20	37.26%	35.37%	14.42%	11.39%	9.73%
	30x30	26.84%	24.29%	6.9%	4.54%	4.25%

15 MV	5x5	24.64%	13.86%	14.15%	26%	22.18%
	10x10	22.22%	6.69%	0.87%	0.67%	0.29%
	20x20	53.25%	42.21%	32.2%	13.28%	16.59%
	30x30	88.39%	70.55%	64.47%	31.44%	6.42%

For 6 MV photon beam energy, the results presented in Table 1 show that the range of beam flatness values for the SH collimator is 0.77% to 6.45%, while for the ML collimator, it is 1.00% to 6.73%. For 15 MV photon beam energy, as shown in Table 2, the range of beam flatness values for the SH collimator is 1.30% to 6.61%, and for the ML collimator, it is 1.04% to 5.29%. Moreover, as shown in Tables 1 and 2, the values of beam flatness increase with increasing depth of measurements. The results are in agreement with those of R. I. Chowdhury et al [20].

The RD in beam flatness values between the SH and ML collimators, as shown in Table 3, are significant, and the highest RD values occur at a depth of maximum dose for both photon beam energies. For the 6 MV photon beam energy, the results indicate a substantial RD in beam flatness associated with various field sizes at d_{max} , where the 5x5 cm² field size shows the highest difference of 66.30%. As the measurement depth increases, these differences generally diminish across all field sizes, with the 30x30 cm² field size demonstrating a significantly lower relative difference of only 4.25%. The 15 MV photon beam energy reveals variable RDs in beam flatness across different field sizes and depths. A significant RD of 24.64% is observed at d_{max} for the 5x5 cm² field, with marked fluctuations noted at deeper levels. The maximum discrepancy recorded for the 15 MV photon beam energy was 88.39% at a 30x30 cm² field size and a depth of 5 cm.

Beam symmetry:

The beam symmetry values for 6 MV and 15 MV photon beam energies were measured at various depths (d_{max} cm, 5 cm, 10 cm, 20 cm, and 30 cm) and field sizes (5x5 cm², 10x10 cm², 20x20 cm², and 30x30 cm²) for both the SH and ML collimators, with the results detailed in Tables 4 and 5, respectively. Additionally, Table 6 presents the RD in beam symmetry values between the SH and ML collimators for the two-photon beam energies of 6 MV and 15 MV.

Table 4: represent the beam symmetry values of 6 MV beam energy at various depths and field sizes for both the SH and ML collimator.

Field size	Collimator type	Depth (cm)				
		d _{max}	5	10	20	30
5x5 cm ²	ML Collimator	1.11	1.25	0.71	0.26	1.08
	Jaw Collimator	0.92	1.02	0.59	0.21	0.91
10x10 cm ²	ML Collimator	0.08	1.08	0.91	0.67	0.24
	Jaw Collimator	0.1	0.9	1.07	0.53	0.19
20x20 cm ²	ML Collimator	0.86	0.73	0.95	0.48	0.71
	Jaw Collimator	1.1	0.92	0.79	0.61	0.59
30x30 cm ²	ML Collimator	0.1	0.24	0.38	0.49	0.7
	Jaw Collimator	0.08	0.19	0.31	0.38	0.52

Table 5: represent the beam symmetry values of 15 MV beam energy at various depths and field sizes for both the SH and ML collimator.

Field size	Collimator type	Depth (cm)				
		d _{max}	5	10	20	30
5x5 cm ²	ML Collimator	0.53	1.1	0.92	1.15	1.85
	SH Collimator	0.38	0.77	0.75	0.84	1.31
10x10 cm ²	ML Collimator	0.78	1.79	1.92	1.19	1.66
	SH Collimator	0.6	1.43	1.45	0.93	1.24
20x20 cm ²	ML Collimator	1.32	1.72	1.13	1.31	1.53
	SH Collimator	1.13	1.45	1.41	1.07	1.24
30x30 cm ²	ML Collimator	1.02	1.04	0.51	1.43	1.11
	SH Collimator	0.78	0.82	0.58	1.2	0.91

Table 6: represent the relative difference in beam symmetry values between the SH and ML collimators for 6 MV and 15 MV photon beam energies.

Beam energy	Field size (cm ²)	Depth (cm)				
		d _{max}	5	10	20	30
6 MV	5x5	32.97	35.29	20.36	31.16	34.18
	10x10	26.09	22.36	27.89	24.53	28.97
	20x20	15.51	17.03	22.05	20.17	20.94
	30x30	26.67	23.66	12.84	17.49	19.8
15 MV	5x5	18.72	20.26	18.46	21.28	17.09
	10x10	22.22	18.18	16.16	23.33	23.26
	20x20	24.49	23.03	18.39	23.85	18.46
	30x30	22.22	23.26	20.29	25.29	29.51

The beam symmetry values of the photon beam with energies of 6 MV and 15 MV and the two types of collimators are within the acceptable limits according to the IEC 60731 standards. Specifically, for the 6 MV photon beam, the symmetry values for the ML collimator vary from 0.08 to 1.25 and from 0.08 to 1.1 for the SH collimator. In contrast, for the 15 MV photon beam, the ML collimator shows symmetry values from 0.51 to 1.92, while the SH collimator ranges from 0.38 to 1.45. The analysis of Tables 4 and 5 reveals no discernible relationship or pattern between symmetry values and variations in field size or depth of measurement, in contrast to the observed patterns associated with flatness values.

The data presented in Table 6 reveal that the RD in beam symmetry values are significant, ranging from 12.84 to 35.29 for the 6 MV photon beam energy, while those for 15 MV range from 16.16 to 29.51. The calculated RD indicate that the 6 MV beam exhibits higher symmetry values than the 15 MV beam across most field sizes, with marked fluctuations in symmetry as a function of depth, particularly notable at d_{max} and depths of 5 cm and 30 cm. Conversely, the 15 MV values demonstrate a trend of decreasing symmetry with increasing depth, particularly evident in larger field sizes.

Beam penumbra:

Tables 7 and 8 present the left and right penumbra measurements of 6 MV and 15 MV photon beams across various field sizes and depths, respectively, for both the ML and Jaw Collimators. Table 9 shows the RD in penumbra values between the ML and SH collimators for both photon beam energies.

Table 7: presented left and right penumbra for 6 MV photon beam across various field sizes and depths.

Field size	Collimator type	Depth (cm)									
		d_{max}		5		10		20		30	
		L. pen	R. Pen	L. pen	R. Pen	L. pen	R. Pen	L. pen	R. Pen	L. pen	R. Pen
5x5 cm ²	ML Collimator	0.5	0.52	0.54	0.54	0.57	0.58	0.63	0.65	0.68	0.67
	SH Collimator	0.62	0.64	0.67	0.68	0.73	0.75	0.81	0.83	0.89	0.9
10x10 cm ²	ML Collimator	0.53	0.55	0.61	0.6	0.68	0.69	0.81	0.8	0.87	0.88
	SH Collimator	0.65	0.66	0.72	0.73	0.82	0.82	1.02	1.01	1.19	1.19
20x20 cm ²	ML Collimator	0.55	0.57	0.61	0.63	0.79	0.81	0.98	1.01	1.21	1.22
	SH Collimator	0.67	0.67	0.77	0.77	0.92	0.95	1.35	1.36	1.62	1.65
30x30 cm ²	ML Collimator	0.57	0.58	0.67	0.67	0.89	0.91	1.12	1.14	1.75	1.78
	SH Collimator	0.64	0.67	0.78	0.8	0.97	1.01	1.21	1.25	1.92	1.89

Table 8: presented left and right penumbra for 15 MV photon beam across various field sizes and depths.

Field size	Collimator type	Depth (cm)									
		d _{max}		5		10		20		30	
		L. pen	R. Pen	L. pen	R. Pen	L. pen	R. Pen	L. pen	R. Pen	L. pen	R. Pen
5x5 cm ²	ML Collimator	0.65	0.64	0.65	0.63	0.7	0.7	0.77	0.76	0.82	0.8
	SH Collimator	0.68	0.69	0.71	0.72	0.76	0.77	0.84	0.86	0.91	0.92
10x10 cm ²	ML Collimator	0.63	0.61	0.65	0.62	0.73	0.73	0.85	0.85	0.94	0.93
	SH Collimator	0.72	0.71	0.74	0.74	0.84	0.84	0.99	0.96	1.09	1.1
20x20 cm ²	ML Collimator	0.84	0.8	0.88	0.88	1.01	1.04	1.12	1.15	1.4	1.38
	SH Collimator	0.88	0.88	0.92	0.93	1.04	1.06	1.16	1.18	1.43	1.42
30x30 cm ²	ML Collimator	0.92	0.92	1.02	1.02	1.09	1.08	1.12	1.14	1.46	1.5
	SH Collimator	0.97	0.97	1.11	1.09	1.12	1.14	1.27	1.28	1.71	1.7

Table 9: represent the relative difference in left and right penumbra between the Jaw collimator (before upgrading) and Multileaf collimator (after upgrading) for the 6 MV and 15 MV photon beam energies.

Beam energy	Field size (cm ²)	Depth (cm)									
		d _{max}		5		10		20		30	
		L. Pen.	R. Pen.	L. Pen.	R. Pen.	L. Pen.	R. Pen.	L. Pen.	R. Pen.	L. Pen.	R. Pen.
6 MV	5x5	21.43	20.69	21.49	22.95	24.62	25.56	25	24.32	26.75	29.3
	10x10	20.34	18.18	16.54	19.55	18.67	17.22	22.95	23.2	31.07	29.95
	20x20	19.67	16.13	23.19	20	15.2	15.91	31.76	29.54	28.98	29.97
	30x30	11.57	14.4	15.17	17.69	8.6	10.42	7.73	9.21	9.26	5.99
15 MV	5x5	4.51	7.52	8.82	13.33	8.22	9.52	8.7	12.35	10.4	13.95
	10x10	13.33	15.15	12.95	17.65	14.01	14.01	15.22	12.15	14.78	16.75
	20x20	4.65	9.52	4.44	5.52	2.93	1.9	3.51	2.58	2.12	2.86
	30x30	5.29	5.29	8.45	6.64	2.71	5.41	12.55	11.57	15.77	12.5

The results in Tables 7 and 8 elucidate the influence of field size, depth of measurement, and photon beam energy on measured penumbra for both photon beam energies. However, Table 9 illustrates the RD between the SH to ML collimator on the measured penumbra which measure the impact of upgrading the LINAC. For both photon beam energies, values of the left and right penumbra consistently increase in correlation with field size and depth due to the geometric divergence of the radiation beam, which results in

increased scattering at the edges. The penumbra width ranges are (0.50 mm – 1.92 mm) for a 6 MV photon beam and (0.61 mm – 1.71 mm) for a photon beam of energy 15MV.

Table 9 provides critical insight into the relative differences in left and right penumbra across various field sizes and depths, comparing measurements obtained with the jaw collimator before the LINAC upgrade to those achieved with the multileaf collimator thereafter, specifically for 6 MV and 15 MV photon beam energies. The relative differences in left and right penumbra values, calculated from beam profiles for jaw and ML collimators at both photon beam energies, are significant and clearly shown in Table 9. For the 6 MV photon beam energy, the minimum value of RD in the right and left penumbra is 5.99%, while the maximum value is 31.76%. However, for the 15 MV photon beam energy, the minimum value of RD in the right and left penumbra is 1.9%, while the maximum value is 17.65%.

Conclusion:

This study effectively analyzes the impact of upgrading the treatment head of the Elekta Precise linear accelerator from the SH to the MLC on the beam profile parameters of 6 MV and 15 MV photon beam energies. The results revealed significant differences in the studied parameters of the beam profile at both beam energies, highlighting the methodological variations introduced by the upgrade. Specifically, there was considerable disagreement in most of the investigated beam profile parameters between the SH and MLC collimators. Notably, the highest discrepancies were observed in measured field size, beam flatness, beam symmetry, and beam penumbra. The relative differences (RD) in beam flatness reached an alarming 88.39%, indicating a substantial alteration that could affect dosimetry and patient treatment outcomes. Additionally, discrepancies of 31.76% in beam penumbra measurements as well as 35.29% in beam symmetry further emphasize the need for careful adjustment and verification of treatment parameters post-upgrade. The percentage difference in measured field size was also notable at 3.3%.

These results emphasize the importance of recommissioning following any significant modifications to ensure the accuracy of data collection, which in turn leads to more precise treatment delivery. Thorough recommissioning is essential for maintaining the integrity of treatment plans and ensuring patient safety. By systematically evaluating these



beam profile parameters after such upgrades, clinical teams can better adapt to changes, optimize treatment effectiveness, and minimize potential risks. Thus, this study provides critical insights that can enhance the reliability of radiotherapy practices in clinical settings.

References:

- [1] Delaney G, Jacob S, Featherstone C, Barton M. The role of radiotherapy in cancer treatment: estimating optimal utilization from a review of evidence-based clinical guidelines. *Cancer*. 2005; 104:1129–1137.
- [2] Begg AC, Stewart FA, Vens C. Strategies to improve radiotherapy with targeted drugs. *Nat Rev Cancer*. 2011; 11:239–253.
- [3] Baskar, R., Lee, K. A., Yeo, R., & Yeoh, K. W. (2012). Cancer and radiation therapy: current advances and future directions. *International journal of medical sciences*, 9(3), 193–199.
- [4] ICRU. ICRU Report 62. Bethesda. MD. 1999. International Commission on Radiation Units and measurements. Prescribing, recording, and reporting photon beam therapy.
- [5] Brahme A., Dosimetric precision requirements in radiation therapy. *ActaRadiol.Oncol.*, 23: 397-91, 1984.
- [6] Dutreix A.: When and how can we improve precision in radiotherapy? *Radiother.Oncol*, 2: 275-92, 1984.
- [7] D. I. Thwaites and J. B. Tuohy, *Back to the future: the history and development of the clinical linear accelerator*, Phys. Med. Biol. 2006.
- [8] Baker, M., & Tannock, I. F. (2010). "Radiotherapy: A Review of Linear Accelerators and their Technologies." *Advances in Technology in Radiation Oncology*, 1(1), 22-31.
- [9] Murray, C., & Orton, C. G. (2011). "Quality Assurance of Radiotherapy Equipment: Linear Accelerators and Associated Systems." *The British Journal of Radiology*, 84(994), 686-697.
- [10] Gross, D. J., & Dempsey, J. F. (2006). "Physicist's Guide to Linear Accelerators." *Journal of Applied Clinical Medical Physics*, 7(1), 29-48.
- [11] Document No. 4513371079803:09©2009 Elekta Ltd.
- [12] Fraass, B., Doppke, K., Hunt, M., Kutcher, G., Starkschall, G., Stern, R., & Van Dyke, J. (1998). American Association of Physicists in Medicine Radiation Therapy Committee Task Group 53: quality assurance for clinical radiotherapy treatment planning. *Medical physics*, 25(10), 1773–1829. <https://doi.org/10.1118/1.598373>
- [13] Abdurraouf M. Aghila, Saad S. Saad, Faraj A. Elmasrub, & Ali A. Alrabee. (2023). Studying and analyzing the impact of upgrading the Elekta Preces Linear accelerator on the percentage depth dose parameters. *مجلة جامعة بني وليد للعلوم الإنسانية والتطبيقية*, 8(5), 617-624. <https://doi.org/10.58916/jhas.v8i5.126>
- [14] International Atomic Energy Agency, *Absorbed dose determination in photon and electron beams*. An International Protocol Technical Report Series No. 277. IAEA, Vienna, 1987.
- [15] International Atomic Energy Agency, *Absorbed Dose Determination in External Beam Radiotherapy: An International Code of Practice for Dosimetry Based on Standards of Absorbed Dose Toi Water*, Technical Report Series no. 398, IAEA, Vienna, 2000.
- [16] International Atomic Energy Agency, *Dosimetry of Small Static Fields Used in External Beam Radiotherapy*, Technical Reports Series No. 483, IAEA, Vienna, 2017.



[17] D Patatoukas, G., Kalavrezos, P., Seimenis, I., Dilvoi, M., Kouloulis, V., Efstathopoulos, E., & Platoni, K. (2018). Determination of beam profile characteristics in radiation therapy using different dosimetric set ups. *Journal of B.U.ON. : official journal of the Balkan Union of Oncology*, 23(5), 1448–1459.

[18] International Atomic Energy Agency, Podgorsak, E. B. (Ed). *Radiation oncology physics: A handbook for teachers and students*, IAEA, Vienna, 2005.

[19] Jbaili, H., Badwi, M. A., Almahmoud, A., & Mhrez, M. (2021). Study of radiation dose distribution for 6MV photon beam product from VARIAN IX linac in case of large fields using BEAMnrc and DOSXYZnrc codes. *Tishreen University Journal for Research and Scientific Studies-Basic Sciences Series*, 43(6), 125–140.

[20] Chowdhury, R. I., Ahmed, R., Rabby, F., Akter, M., & Rahman, M. (2024). Beam profile characteristics of a Varian linear accelerator across different photon energy levels. *International Journal of Science and Research Archive*. 12(02), 1072-1082.

